PNAS PLUS

GIV/Girdin activates Gαi and inhibits Gαs via the same motif

Vijay Gupta[a], Deepali Bhandari[a,1], Anthony Leyme[b], Nicolas Aznar[c], Krishna K. Midde[c], I-Chung Lo[a], Jason Ear[a,c], Ingrid Niesman[a], Inmaculada López-Sánchez[c], Juan Bautista Blanco-Canosa[d], Mark von Zastrow[e], Mikel Garcia-Marcos[b], Marilyn G. Farquhar[a,2], and Pradipta Ghosh[a,c,2]

[a]Department of Cellular and Molecular Medicine, University of California, San Diego, La Jolla, CA 92093; [b]Department of Biochemistry, Boston University School of Medicine, Boston, MA 02118; [c]Department of Medicine, University of California, San Diego, La Jolla, CA 92093; [d]Department of Chemistry and Molecular Pharmacology, Institute for Research in Biomedicine, 08028 Barcelona, Spain; and [e]Department of Psychiatry, University of California, San Francisco, CA 94158

Contributed by Marilyn G. Farquhar, June 20, 2016 (sent for review November 28, 2015); reviewed by Kendall J. Blumer, Vladimir L. Katanaev, and David P. Siderovski

We previously showed that guanine nucleotide-binding (G) protein α subunit (Gα)-interacting vesicle-associated protein (GIV), a guanine-nucleotide exchange factor (GEF), transactivates Gα activity-inhibiting polypeptide 1 (Gαi) proteins in response to growth factors, such as EGF, using a short C-terminal motif. Subsequent work demonstrated that GIV also binds Gαs and that inactive Gαs promotes maturation of endosomes and shuts down mitogenic MAPK–ERK1/2 signals from endosomes. However, the mechanism and consequences of dual coupling of GIV to two G proteins, Gαi and Gαs, remained unknown. Here we report that GIV is a bifunctional modulator of G proteins; it serves as a guanine nucleotide dissociation inhibitor (GDI) for Gαs using the same motif that allows it to serve as a GEF for Gαi. Upon EGF stimulation, GIV modulates Gαi and Gαs sequentially: first, a key phosphomodification favors the assembly of GIV–Gαi complexes and activates GIV's GEF function; then a second phosphomodification terminates GIV's GEF function, triggers the assembly of GIV–Gαs complexes, and activates GIV's GDI function. By comparing WT and GIV mutants, we demonstrate that GIV inhibits Gαs activity in cells responding to EGF. Consequently, the cAMP→PKA→cAMP response element-binding protein signaling axis is inhibited, the transit time of EGF receptor through early endosomes are accelerated, mitogenic MAPK–ERK1/2 signals are rapidly terminated, and proliferation is suppressed. These insights define a paradigm in G-protein signaling in which a pleiotropically acting modulator uses the same motif both to activate and to inhibit G proteins. Our findings also illuminate how such modulation of two opposing Gα proteins integrates downstream signals and cellular responses.

heterotrimeric G proteins | cAMP | cancer invasion | growth factor receptor tyrosine kinase | guanine nucleotide dissociation inhibitor

The guanine nucleotide-binding (G) protein α subunit (Gα)-interacting vesicle-associated protein (GIV, also known as "Girdin") is a multimodular signal transducer and a nonreceptor guanine nucleotide exchange factor (GEF) for Gα activity-inhibiting polypeptide 1 (Gαi) (1). GIV binds G proteins and other signaling molecules and thereby couples G proteins to diverse signaling pathways [e.g., Akt and PI3K (2, 3)] and cell functions. Mechanistically, the best-studied aspect of GIV is its role in coupling growth factor signaling to Gi signaling (reviewed in refs. 4 and 5): Upon stimulation with growth factors such as EGF, GIV uses an SH2-like module to bind directly to the autophosphorylated cytoplasmic tail of the EGF receptor (EGFR) (6) and recruits and transactivates Gi in the vicinity of ligand-activated receptors (7). GIV is also directly phosphorylated by receptor and nonreceptor tyrosine kinases, allowing GIV to bind and activate PI3K directly (8) and enhance Akt signaling (2, 3) to trigger cell migration. Upon endocytosis of EGFR, GIV binds Gαs and follows EGFR to endosomes (9) where it facilitates down-regulation of EGFR and limits cell proliferation. Thus GIV is ubiquitously expressed (10), can be recruited to different subcellular compartments (reviewed in ref. 4), binds to both Gαi and Gαs (9–11), and affects a number of important physiologic and pathologic processes.

Mechanistically, it is known that GIV triggers the migration of diverse cell types in a variety of contexts, e.g., tumor cell motility and invasion, among others (reviewed in ref. 5). Migration is triggered when GIV activates Gαi via an evolutionarily conserved Gα-binding and activating (GBA) motif and releases "free" Gβγ heterodimers, which stimulate motogenic signals such as the PI3K–Akt pathway (reviewed in ref. 5). However, selective ablation of GIV's GBA motif not only disables cells' ability to migrate in response to a stimulus but also results in an unexpected gain in phenotype, i.e., cells begin to proliferate (11–13). How GIV's GBA motif actively suppresses cell proliferation remained unclear. Subsequent work showed that GIV also binds Gαs; the GIV–Gαs interaction and the presence of Gαs in an inactive state that promotes maturation of endosomes shuts down the mitogenic MAPK–ERK1/2 signals from endosomes and suppresses cell proliferation (9). In the absence of Gαs or in cells expressing a constitutively active mutant Gαs, EGFR stays longer in endosomes, MAPK–ERK1/2 signals are enhanced, and cells proliferate (9).

Significance

Guanine nucleotide-binding (G) protein α subunit (Gα)-interacting vesicle-associated protein (GIV)/Girdin has previously been shown to serve as a guanine nucleotide exchange factor (GEF) for the Gα activity-inhibiting polypeptide 1 (Gαi) via a conserved motif in its C terminus. Here we show that this motif serves as a guanine nucleotide dissociation inhibitor (GDI) for Gαs. Sequential phosphorylation of two serine residues that flank this motif by two kinases, cyclin-dependent kinase 5 and PKCθ, ensures that GIV exerts its GEF and GDI activities on Gαi and Gαs, respectively, in a temporally and spatially segregated manner. Through its bifunctional role as GEF and GDI, GIV serves as a pleiotropically acting G-protein modulator that integrates, reinforces, and compartmentalizes signals downstream of both growth factors and G proteins and orchestrates migration–proliferation dichotomy.

Author contributions: V.G., D.B., A.L., N.A., K.K.M., I.-C.L., J.E., I.L.-S., M.G.-M., M.G.F., and P.G. designed research; V.G., D.B., A.L., N.A., K.K.M., I.-C.L., J.E., I.N., I.L.-S., M.G.-M., and P.G. performed research; J.B.B.-C., M.v.Z., M.G.F., and P.G. contributed new reagents/analytic tools; V.G., D.B., A.L., N.A., K.K.M., I.-C.L., J.E., I.N., I.L.-S., M.v.Z., M.G.-M., M.G.F., and P.G. analyzed data; M.G.F. and P.G. supervised all parts of the work; and M.G.-M., M.G.F., and P.G. wrote the paper.

Reviewers: K.J.B., Washington University School of Medicine; V.L.K., University of Lausanne; and D.P.S., West Virginia University.

The authors declare no conflict of interest.

[1]Present address: Department of Chemistry and Biochemistry, California State University, Long Beach, CA 90840.

[2]To whom correspondence may be addressed. Email: mfarquhar@ucsd.edu or prghosh@ucsd.edu.

This article contains supporting information online at www.pnas.org/lookup/suppl/doi:10.1073/pnas.1609502113/-/DCSupplemental.

Although the published work led us to conclude that a main function of GIV is to orchestrate the migration–proliferation dichotomy by enhancing cell migration and inhibiting mitosis (9, 11, 12) and that GIV must dually couple to both Gαi and Gαs to orchestrate such dichotomy, several questions remained unanswered. For example, what determines GIV's preference for one or the other G protein, and how does dual coupling to Gαi and Gαs impact signals downstream of both G proteins and receptor tyrosine kinases and cellular responses to growth factors? Here we show that GIV accomplishes the migration–proliferation dichotomy by interacting sequentially with and paradoxically modulating the nucleotide exchange of two different G proteins with opposing roles: GIV uses an evolutionarily conserved bifunctional GBA motif that serves as a GEF to activate Gαi at the plasma membrane (PM) and trigger cell migration and that serves as a guanine nucleotide dissociation inhibitor (GDI) to inhibit Gαs at endosomes and limit cell proliferation. Such bifunctional GEF and GDI activities were previously reported for the synthetic KB-752 peptide (14, 15), whose sequence led to the identification of the GBA motif in GIV and other members of the GIV family (reviewed in ref. 5). By identifying the naturally occurring bifunctional sequence in GIV, this study illustrates a paradigm in paradoxical G-protein signaling in which, depending on the G-protein substrate, a versatile modulator uses the same motif to accelerate or inhibit nucleotide exchange. We also define the key phosphomodifications that trigger the GEF or GDI functions of GIV, thereby ensuring robustness amid versatility.

Results

GIV Binds Sequentially to Two G Proteins, First to Gαi and then to Gαs. Work to date has shaped the current working model (Fig. 1*A*) for how GIV coordinates the cellular response to EGF by binding two Gα subunits at two places in cells: GIV interacts with Gαi at the PM (7) and with Gαs on endosomes (9). To determine if GIV can bind both G proteins at any time or binds sequentially to one or the other, we performed proximity ligation assays (PLA) (16) to detect in situ GIV–Gαi3 (Fig. 1*B*) and GIV–Gαs (Fig. 1*C*) complexes in HeLa cells. PLA signals between endogenous GIV and both Gαi3 and Gαs were detected most prominently after EGF stimulation, indicating that they interact [i.e., the maximum distance between the two is ≤30–40 nm (16)] and that such interactions are ligand dependent. A quantitative analysis of the abundance of GIV–Gαi and GIV–Gαs complexes, as determined by the number of PLA dots per cell, revealed that GIV interacts with Gαi and Gαs sequentially: The assembly of GIV–Gαi complexes is triggered within 5 min after EGF stimulation (t5) (see the graph in Fig. 1*B*). Although some GIV–Gαs complexes were detected in starved cells, their ligand-dependent assembly is triggered later, at 15 min after EGF stimulation (t15), and peaks at 30 min after EGF stimulation (t30), and their disassembly occurs by 60 min after EGF stimulation (t60) (see the graph in Fig. 1*C*). The sequential nature of in situ interactions of GIV with Gαi/s was also confirmed biochemically using protein–protein interaction assays (Fig. 1*D*) by analyzing endogenous Gαi/s proteins bound to a GST-tagged C-terminal fragment of GIV (GST-GIV-CT) expressed in

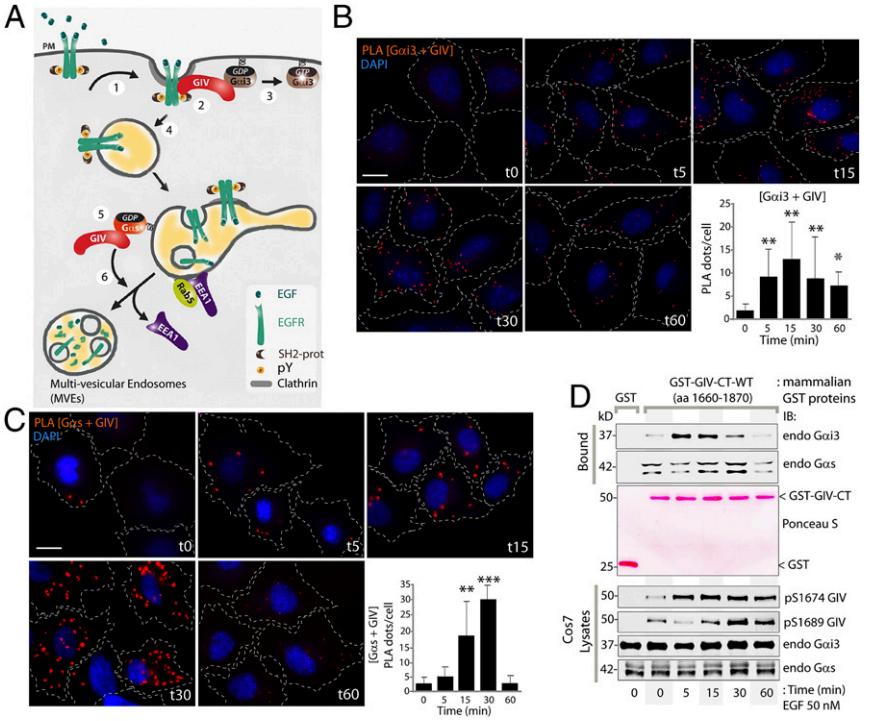

Fig. 1. Upon EGF stimulation GIV binds Gαi3 and Gαs in a sequential manner. (*A*) Schematic summarizing GIV's interactions with Gαi3 and Gαs at various steps in EGFR signaling and trafficking (modified from ref. 9). Upon EGF stimulation, GIV is recruited to the PM (step 1), assembles an EGFR–GIV–Gαi3 complex at the PM (step 2), activates Gαi3 (step 3), and prolongs the association of EGFR with the PM. Upon internalization, EGFR traffics to APPL endosomes (step 4) and then to EEA1 endosomes where GIV binds inactive Gαs (step 5), promoting dissociation of EEA1 and endosome maturation to multivesicular endosomes (step 6) to facilitate EGFR down-regulation, thus shutting off endosome-based proliferative signaling. (*B* and *C*) Serum-starved (0.2% FBS, overnight) HeLa cells were stimulated with EGF at the indicated time points and were fixed and analyzed for interactions between GIV and Gαi3 (*B*) or GIV and Gαs (*C*) by in situ PLA (red). Nuclei are stained with DAPI (blue). Cell boundaries were traced with interrupted lines by superimposing bright-field microscopy images. Results are expressed as mean ± SEM; $n = 3$. (Scale bar, 15 μm.) (*Lower Right*) The number of PLA dots per cell was quantified from a total of 25–30 cells per experiment. (*D*) Cos7 cells expressing GST-GIV-CT (amino acids 1660–1870) were stimulated with EGF at the indicated time points and were lysed and incubated with glutathione-Sepharose beads. (*Top*) Bound proteins were analyzed for endogenous Gαi3 and Gαs by immunoblotting (IB). (*Middle*) Equal loading of GST and GST-GIV-CT proteins was confirmed by Ponceau-S staining. (*Bottom*) Cell lysates were analyzed for pS1674-GIV, pS1689-GIV, Gαi3, and Gαs by immunoblotting and were quantified using LI-COR Odyssey (Fig. S1). $^{*}P < 0.05$, $^{**}P < 0.01$, $^{***}P < 0.001$.

Cos7 cells. GIV preferentially bound Gαi by t5, and the interaction decreased by t30 (Fig. 1*D* and Fig. S1). Consistent with our observation using PLA assays (Fig. 1*C*), GIV maximally bound Gαs at t30 (Fig. 1*D* and Fig. S1). FRET-based assays using a previously validated CFP-tagged GIV-CT probe (7) also confirmed that GIV–Gαs interaction occurs at t30 on vesicular structures, presumably endosomes (Fig. S2). Taken together, these results demonstrate that upon EGF stimulation GIV–Gαi complexes form first, followed by GIV–Gαs complexes, suggesting that the shift in the composition of GIV–Gα complexes may be orchestrated by some sequential regulatory event(s).

GIV's Ability to Bind Gαi3 and Gαs Sequentially Is Regulated by Two Key Phosphomodifications. It is noteworthy that GIV's C terminus (GIV-CT; amino acids 1660–1870) containing the evolutionarily conserved GBA motif (amino acids 1678–1694) (Fig. 2*A*) that binds and activates Gαi could recapitulate the sequential profile of the binding of full-length GIV to Gαi and Gαs (Fig. 1*D*). Based on this observation, we hypothesized that phosphorylation of one or more key serine/threonine residues that flank the GBA motif may regulate GIV's ability to bind both Gαi and Gαs sequentially. In this regard, we recently reported that cyclin-dependent kinase 5 (CDK5) phosphorylates S1674 just upstream of GIV's GBA motif within seconds to minutes after EGF stimulation and triggers GIV to bind both Gαi and Gαs, albeit with a higher affinity for Gαi (11). Another kinase, PKCθ, phosphorylates S1689 just downstream of the GIV's GBA motif at approximately t15–t30 and terminates GIV's ability to bind and/or activate Gαi (13). Analysis of these key phosphomodifications on the G-protein–bound GST-GIV-CT protein (Fig. 1*D*, *Bottom*) demonstrated that GIV-CT was phosphorylated at S1674 by t5, coinciding with maximal binding to Gαi3. Phosphorylation at S1689 peaked at t30, coinciding with a selective loss of GIV's ability to bind Gαi and enhanced binding to Gαs (Fig. 1*D*). Because phosphorylation at S1674 alone increased GIV's binding to both Gα subunits, but GIV continues to bind Gαi at a higher affinity (11), we reasoned that this phosphoevent cannot account for the shift in GIV's preference from Gαi to Gαs. Instead the shift is likely to be brought about by the second phosphoevent at S1689, because phosphorylation at that site disrupts binding to Gαi without affecting binding to Gαs.

To investigate if phosphorylation of S1674 and/or S1689 affects GIV's ability to bind Gαi/s, we generated several phosphomimicking mutants of full-length GIV or GST-tagged GIV-CT by replacing serine (S) with aspartate (D) at S1674 alone (74D), at S1689 alone (89D), or at both sites (74D/89D, hereafter "DD") and tested their ability to bind Gαi3 and Gαs in a series of protein–protein interaction assays (Fig. 2 *B*–*E*). First we immunoprecipitated FLAG-tagged Gαi3 (Fig. 2*B*) or Gαs (Fig. 2*C*) and looked for binding to Myc-tagged full-length GIV-WT and mutants. In the

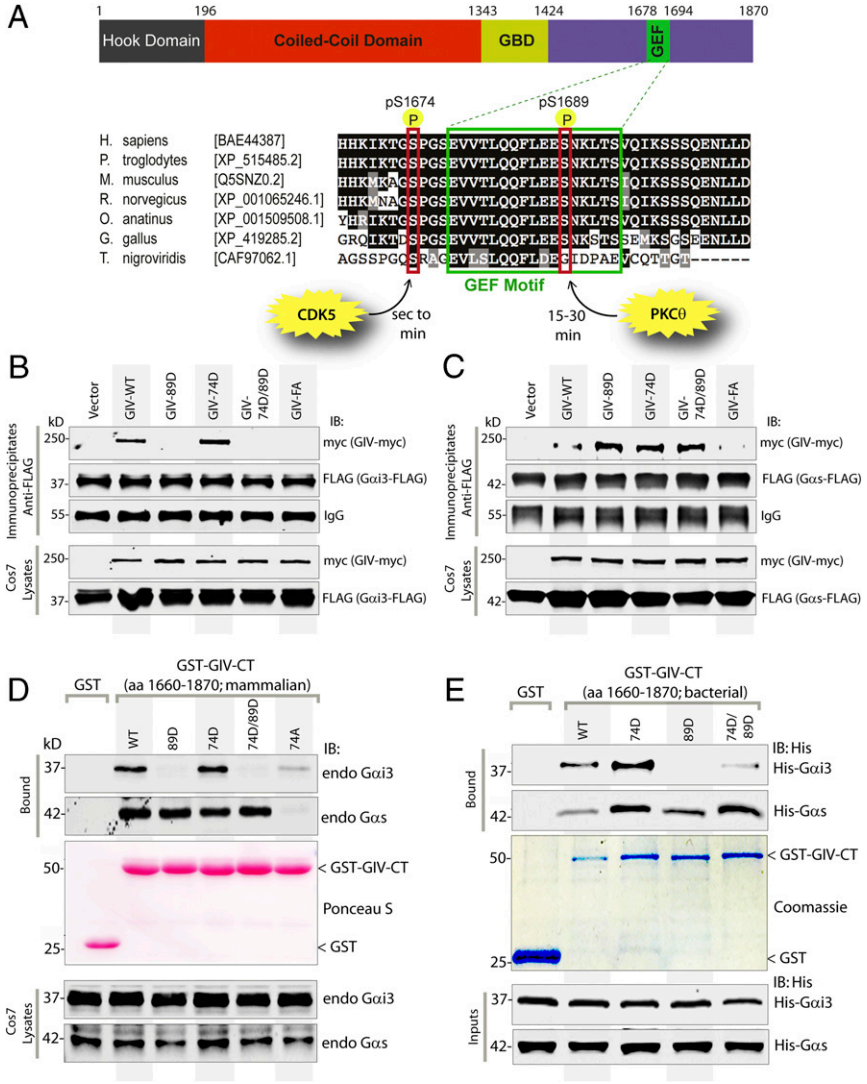

Fig. 2. Sequential phosphorylation of GIV by CDK5 and PKCθ triggers sequential GIV–Gαi3 and GIV–Gαs interactions. (*A*) Schematic of the domain architecture of GIV and sequence alignment of its C-terminal GEF motif. (*Upper*) Various domains of GIV are shown. Residue numbers marking the boundaries of each domain are shown. (*Lower*) The sequence encompassing the GEF motif (green rectangle) and surrounding residues was aligned among various species (accession numbers are shown in brackets) using ClustalW. Conserved residues are shaded in black, and similar residues are shaded in gray. The two phosphorylated residues (S1674 and S1689 in human GIV) that respectively activate (11) and inactivate (13) the GEF function are boxed in red. The timing of these phosphoevents after EGF stimulation and the kinases responsible for these two regulatory phosphoevents [CDK5 (11) and PKCθ (13)] are shown also. (*B* and *C*) Immunoprecipitation was carried out with anti-FLAG antibody on equal aliquots of lysates of Cos7 cells coexpressing Gαi3-FLAG (*B*) or FLAG-Gαs (C) with full-length Myc-tagged GIV (WT and mutants), followed by incubation with protein-G Sepharose beads. Immunoprecipitates (*Upper*) and lysates (*Lower*) were analyzed for GIV-Myc and Gαi3-FLAG (*B*) or Gαs-FLAG (*C*) by immunoblotting. (*D*) Lysates of Cos7 cells expressing WT or mutant GST-GIV-CT were incubated with glutathione-Sepharose beads. Bound proteins (*Upper*) and lysates (*Lower*) were analyzed by immunoblotting for endogenous (endo) Gαi3 and Gαs and were quantified using band densitometry (Fig. S3*A*). Equal loading of GST proteins was confirmed by Ponceau-S staining. (*E*) Equimolar amounts of purified His-Gαi3 (*Upper*) or His-Gαs (*Lower*) were incubated with GST or GST-GIV-CT proteins (WT and mutants) immobilized on glutathione-Sepharose beads (Coomassie). Bound His-Gαi3 or His-Gαs was analyzed by immunoblotting using anti-His mAb and was quantified using band densitometry (Fig. S3*B*). Equal loading of inputs was confirmed by immunoblotting using anti-His mAb.

case of Gαi3 (Fig. 2*B*), binding was detected with GIV-WT and was slightly augmented with the phosphomimetic 74D mutant, exactly as reported previously (11). In keeping with previous work (13), binding was undetectable with the phosphomimetic 89D mutant (Fig. 2*B*). Binding also was undetectable with the double-phosphomimetic DD mutant, indicating that inhibitory phosphorylation at S1689 likely overrides the augmentation brought about by phosphorylation at S1674. Gαs binding to GIV-74D was enhanced compared with GIV-WT (Fig. 2*C*), exactly as reported previously (11). However, unlike Gαi, Gαs continued to bind GIV-89D and GIV-DD mutants, indicating that dually phosphorylated GIV can bind Gαs exclusively. Similar results were obtained when we expressed various phosphomimetic GST-GIV-CT mutants in mammalian cells and tested their ability to bind endogenous Gαi3 and Gαs (Fig. 2*D* and Fig. S3*A*). Once again, the GIV-89D and GIV-DD mutants exclusively bound Gαs but not Gαi. The GEF-deficient F1685A (GIV-FA) mutant (Fig. 2 *B* and *C*) (1) or the phosphorylation-deficient S1674A (hereafter, "74A") mutant (Fig. 2*D*) (11) showed little to no binding to either Gαi3 or Gαs, indicating that an intact GEF motif is required for both interactions. Finally, we expressed the same mutant GST-GIV-CT constructs in bacteria and carried out in vitro pulldown assays with recombinant 6×His-tagged Gαi3 or Gαs (Fig. 2*E* and Fig. S3*B*). Once again, compared with GIV-WT, binding to GIV-74D was enhanced for both Gαi and Gαs, whereas only Gαs bound to the GIV-89D and GIV-DD mutants. It is noteworthy that the increase in the binding of both G proteins to GIV-74D (relative to GIV-WT) is not appreciated when the pulldown assays are carried out on cell lysates (Fig. 2*D* and Fig. S3*A*) rather than on purified recombinant proteins (Fig. 2*E* and Fig. S3*B*). This discrepancy likely stems from the S1674 residue in GIV-CT-WT being abundantly phosphorylated (~35%) in cells at steady state, as determined by mass spectrometry (11). These findings demonstrate that, despite key differences in how phosphorylation of two serine residues (1674 and 1689) that flank the GEF motif may affect GIV's ability to bind Gαi vs. Gαs, the binding nonetheless relies on the presence of an intact GEF motif. These findings also support the hypothesis that sequential phosphorylation, first at S1674 and then at S1689, is sufficient to orchestrate a shift in the composition of GIV–Gα complexes from Gαi3 to Gαs. It is phosphorylation at S1674 that serves as a key determinant of GIV's ability to bind Gαi and Gαs in vitro, but it is phosphorylation at S1689 that reduces GIV's ability to bind Gαi without affecting its ability to bind Gαs in vivo. These results also provide a set of tools (specific mutants) to interrogate further GIV's interplay with the two G proteins: GIV-WT physiologically binds both G proteins sequentially, GIV-FA binds neither, and GIV-DD is the physiologically relevant mutant that is expected to bind Gαs selectively and maximally, but not Gαi. No mutants could be designed that selectively bind Gαi. Thus we used the DD and FA mutants as the GDI-proficient and GDI-deficient GIV mutants, respectively, and analyzed them alongside GIV-WT in all subsequent assays. GIV-FA, rather than the nonphosphorylatable 74A mutant, was the preferred GDI-deficient mutant, either alone or in combination, for three reasons: (*i*) it has been characterized extensively in prior work, including work investigating the GIV–Gαs interaction (9), and therefore preserves continuity and enables comparisons; (*ii*) its specificity for disrupting GIV–Gα interactions while allowing binding to receptor or other downstream effectors (6) has been confirmed; and (*iii*) its design and effect on GIV–Gα interaction are guided and explained by a strong structural rationale, whereas the disruptive effect of the 74A mutation remains incompletely understood (11).

GIV Serves as a GDI for Gαs via the Same Motif It Uses to Activate Gαi. To determine the consequence of GIV–Gαs interaction and the impact of GIV phosphorylation on Gαs activity, we carried out enzymatic assays using recombinant, bacterially expressed WT and mutant His-GIV-CT (Fig. 3*A*) and His-Gαs proteins in vitro. When we measured the steady-state GTPase activity of Gαs alone or in the presence of different concentrations of His-GIV-CT WT or various phosphomimetic mutants (74D, 89D, or DD) at a fixed time point (t15), we found that although all inhibited steady-state Gαs GTPase activity in a dose-dependent manner, the dual phosphomimetic DD mutant was significantly more efficient than GIV-WT or any of the other mutants at each concentration tested (from ~20–25% to ~50% inhibition at 2 μM) (Fig. 3*B*). No significant difference was observed between GIV WT and either of the two single mutants, 74D or 89D. Time-course experiments (Fig. 3*C*) confirmed these inhibitory effects and validated that the dose-dependence experiments were carried out under conditions in which the GTPase activity is linear, therefore reflecting bona fide changes in activity rates. To mitigate concerns about the integrity and purity of His-tagged GIV-CT used in these experiments, we synthesized WT and dual phosphomimetic GIV-DD peptides (*SI Experimental Procedures*) and tested their ability to inhibit Gαs in steady-state GTPase assays. Much like the purified His-tagged proteins, WT peptide showed a weak inhibitory effect (~20% at 5 μM), whereas the DD mutant peptide was significantly more potent (~50% at 5 μM) (Fig. 3*D*). Although diminished steady-state GTPase activity of Gαs suggests inhibition of nucleotide exchange, the reduced activity also could be caused by inhibition of the intrinsic rate of GTP hydrolysis. We ruled out the latter possibility by carrying out GTPγS-binding assays that directly measure nucleotide exchange rates. These experiments showed that WT peptide reduced GTPγS binding by ~20%, and the DD mutant peptide inhibited binding by ~50%, whereas the control FA mutant peptide, which does not bind Gαs (Fig. 2 *B* and *C*), had no effect (Fig. 3*E*). Taken together, these results indicate that GIV has modest GDI activity on Gαs and that this activity is enhanced by dual phosphorylation at S1674 and S1689.

To determine if GIV functions as a GDI and inhibits Gαs activity in HeLa cells, we used two different approaches, immunofluorescence on fixed cells and fluorescence live-cell imaging using two different conformation-specific anti-Gαs antibodies. For immunofluorescence we used a commercially obtained mouse monoclonal IgG that specifically recognizes the active GTP-bound conformation of Gαs (anti–Gαs-GTP) (Fig. 3*F*). In control cells, no significant Gαs activity was detected either before or after ligand stimulation, indicating either that Gαs is not activated after EGF stimulation or that its activity is efficiently suppressed by some modulator for sustained periods of time. In GIV-depleted cells [80–85% depletion of endogenous GIV by shRNA sequence targeting the 3′ UTR (*SI Experimental Procedures* and Fig. S4)] Gαs activity was easily detected exclusively after ligand stimulation (Fig. 3*F*, *Lower*), indicating that GIV is required for the suppression of Gαs activity. A similar pattern also was observed by live-cell imaging using the extensively well-validated Gαs conformational biosensor, nanobody Nb37-GFP that binds and helps detect the nucleotide-free intermediate during Gαs activation (17). Little or no Gαs activity was seen in control HeLa cells responding to EGF; in GIV-depleted cells, however, a significant increase in Gαs activity was seen on vesicular structures that are likely to be endosomes (Fig. 3 *G* and *H* and Movies S1 and S2). These findings demonstrate that GIV is required for the inhibition of Gαs activity after EGF stimulation. Next we carried out similar analyses on HeLa cell lines stably expressing GIV-WT, GIV-DD (phosphomimetic, GDI-proficient), and GIV-FA (GDI-deficient) mutants at physiologic levels (Fig. S4). In GIV-WT and GIV-DD Hela cells responding to EGF little or no Gαs activity was seen; however, in GIV-FA Hela cells a significant increase in Gαs activity was seen on vesicular structures that are likely to be endosomes at t20 (Fig. 3 *I* and *J* and Movies S3–S5). These results obtained in live cells using conformation-sensitive antibodies are in agreement with our in vitro enzymatic assays: Both approaches point to GIV's GDI function having a role in the inhibition of Gαs activity.

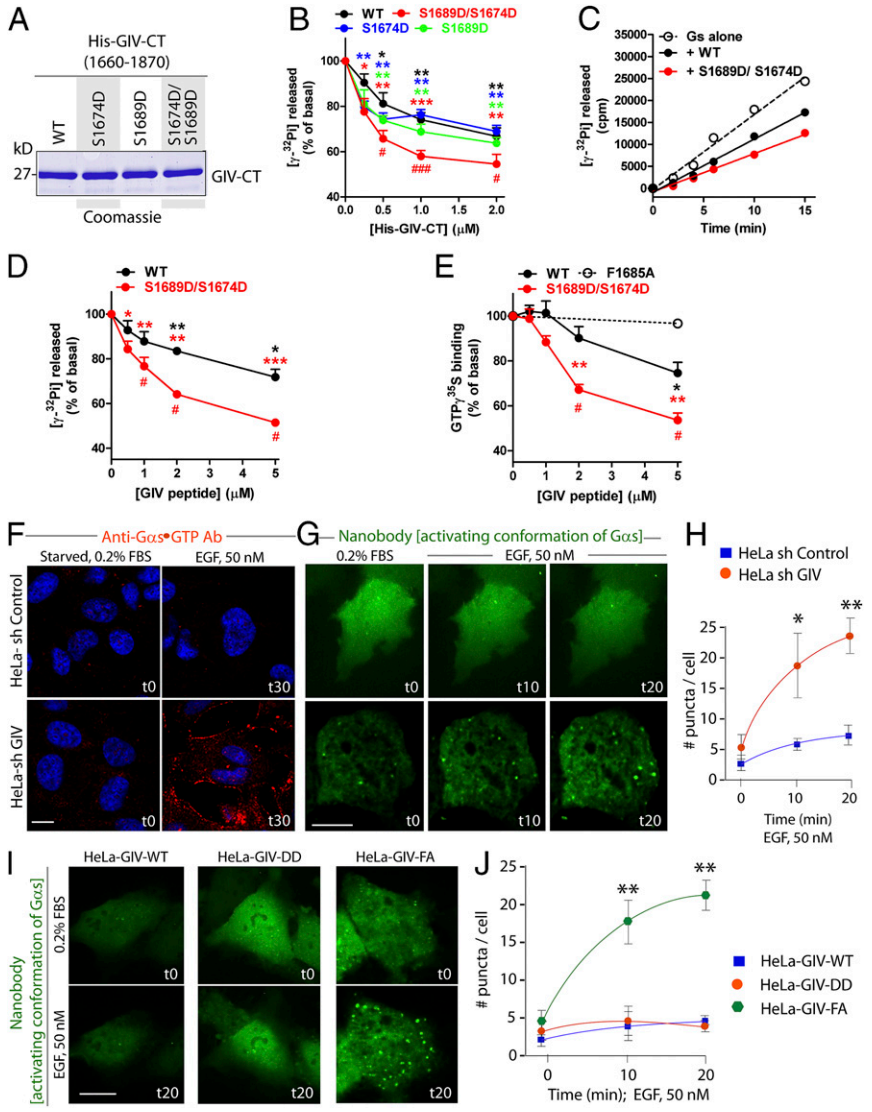

Fig. 3. GIV serves as a GDI for Gαs. (*A*) His-tagged WT C-terminal (amino acids 1660–1870; His-GIV-CT WT) and various phosphomimetic mutants of GIV were purified from bacteria, analyzed by SDS/PAGE, and stained with Coomassie blue. (*B*) The steady-state GTPase activity of His-Gαs (50 nM) was determined at t15 in the presence of increasing concentrations of purified His-GIV-CT WT (black), S1674D (blue), S1689D (green), or S1674D/S1689D (red). Gαs activity is expressed as percent of the steady-state GTPase activity of Gαs alone in the absence of His-GIV-CT protein. Results are expressed as ± SEM; $n = 3$. $^{*}P < 0.05$, $^{**}P < 0.01$, $^{***}P < 0.001$ compared with no GIV; $^{\#}P < 0.05$, $^{\#\#}P < 0.01$ compared with GIV WT at the same concentration. (*C*) The steady-state GTPase activity of His-Gαs (50 nM) was determined by measuring (in counts per minute) the release of radiolabeled phosphate at different time points in the absence (open circles) or presence of 1 μM purified His-GIV-CT WT (solid black circles) or His-GIV-CT S1674D/S1689D (solid red circles). One experiment representative of three is shown. (*D*) The steady-state GTPase activity of His-Gαs (50 nM) was determined at t15 in the presence of increasing concentrations of a synthetic GIV-derived peptide (amino acids 1671–1705) of WT sequence (black) or containing the S1674D/S1689D mutations (red). Gαs activation is expressed as percent of the steady-state GTPase activity of Gαs alone in the absence of any peptide. Results are expressed as ± SEM; $n = 3$. $^{*}P < 0.05$, $^{**}P < 0.01$, $^{***}P < 0.001$ compared with no GIV; $^{\#}P < 0.05$ compared with GIV WT at the same concentration. (*E*) GTPγS binding by His-Gαs (50 nM) was determined by measuring the incorporation of ^{35}S-radiolabeled nucleotide at t15 in the presence of increasing concentrations GIV-derived peptide (amino acids 1671–1705) of WT sequence (black), containing the DD mutations (red), or the FA mutation (G-protein binding–deficient negative control; dashed line). Results are expressed as ± SEM; $n = 3$. $^{*}P < 0.05$, $^{**}P < 0.01$ compared with no GIV; $^{\#}P < 0.05$ compared with GIV WT at the same concentration. (*F*) Serum-starved control (shControl) and GIV-depleted (shGIV) HeLa cells were stimulated with 50 nM EGF for 30 min and then were fixed and stained for active Gαs using anti-Gαs·GTP (red) and DAPI (to stain the nucleus; blue) and were analyzed by confocal microscopy. (Scale bars, 10 μm.) (*G*–*J*) Control (shControl) and GIV-depleted (shGIV) HeLa cells (*G* and *H*) or HeLa cells stably expressing GIV-WT or the DD or FA mutants (*I* and *J*) expressing GFP-tagged anti–Gαs-GTP (activating) conformation-specific nanobodies were serum starved overnight, stimulated with 50 nM EGF, and analyzed by live-cell imaging using a Leica scanning disk microscope for 20 min. Freeze frames from representative cells are shown in *G* and *I*. Bright puncta indicate active Gαs. (Scale bars, 10 μm.) Graphs in *H* and *J* show the average number of puncta per cell (*y* axis) at the indicated time points (*x* axis) in the experiments shown in *G* and *I*, respectively. Results are expressed as ± SEM; $n = 3$. $^{*}P < 0.05$, $^{**}P < 0.01$.

GIV Suppresses the cAMP→PKA→cAMP Response Element-Binding Protein Pathway via Its Ability to Inhibit Gαs. Next we analyzed the impact of GIV's GDI function on signaling pathways downstream of Gαs, i.e., the cAMP→PKA→cAMP response element-binding protein (CREB) pathway. First, we assessed cellular levels of cAMP using a previously well-characterized ^{T}Epac^{VV} FRET probe (described in *SI Experimental Procedures*) that detects submicromolar changes in the second messenger (18). We found that in the presence of GIV (shControl HeLa cells), EGF stimulation was accompanied by suppression of cellular cAMP in a bimodal pattern, as determined by the increase in intramolecular FRET (Fig. 4*A*). An early wave of cAMP suppression was observed at approximately t5–t6, followed by a late wave of suppression at approximately t15–t45 (Fig. 4*A*); both events are delayed compared with the rapid (i.e., within a few seconds) suppression observed with the same FRET probes in the setting of canonical activation of Gi by Gi-coupled receptors (GPCRs) (19). However, as we reported previously (7), in the absence of GIV (i.e., in GIV-depleted cells) no suppression of cAMP was observed in response to EGF. We hypothesized that the first wave of suppression is a consequence of GIV's ability to bind and activate Gαi, whereas the later wave is a consequence of GIV's ability to bind and inhibit Gαs. To test this hypothesis, cAMP was assessed by FRET in HeLa cells stably expressing GIV-WT or the GDI-proficient/GEF-deficient GIV-DD or GDI/GEF-deficient GIV-FA mutants. We found that GIV-WT and GIV-FA Hela cells showed a pattern similar to that observed in shControl and shGIV cells, respectively (Fig. 4*B*). GIV-DD Hela cells differed from both, in that they failed to suppress cAMP early on but suppressed it efficiently later (Fig. 4*B*). The patterns of changes observed in cAMP are consistent with GIV's role as a GEF for Gαi early and as a GDI for Gαs later in cells responding to EGF.

Further downstream, GIV-depleted cells also showed elevated levels of cellular PKA activity, as determined by an antibody that recognizes the abundance of phosphosubstrates of the kinase (Fig. 4*C*) and, more specifically, by analyzing the levels of phosphorylated CREB and the closely related substrate, activating transcription factor-1 (ATF1) (Fig. 4*E* and Fig. S5*A*). HeLa cells stably expressing the GDI-proficient GIV-DD mutant effectively suppressed PKA activity (Fig. 4*D*) and phosphorylation of CREB and

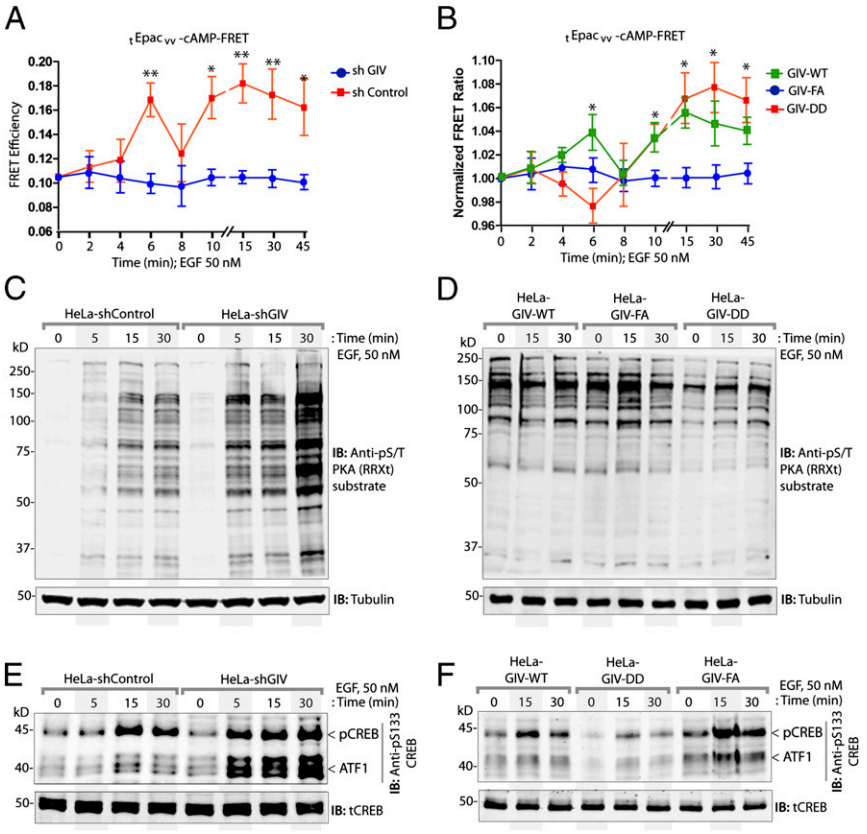

Fig. 4. GIV inhibits the Gαs–GTP→cAMP→PKA→CREB pathway. (*A* and *B*) Control (shControl) and GIV-depleted (shGIV) HeLa cells (*A*) or GIV-WT, GIV-DD, or GIV-FA Hela cell lines (*B*) expressing the $_t$Epac$_{vv}$-cAMP FRET probe were serum starved (0.2% FBS) and subsequently stimulated with 50 nM EGF and analyzed for ratiometric FRET imaging using a confocal microscope (increase in cAMP = loss of FRET, and vice versa). Graphs display the change in FRET efficiency (*y* axis) over time (*x* axis). Results are expressed as ± SEM; $n = 3$. $^*P < 0.05$, $^{**}P < 0.01$. (*C* and *D*) Serum-starved control (shControl) or GIV-depleted (shGIV) HeLa cell lines (*C*) or GIV-depleted HeLa cells stably expressing GIV-WT, GIV-DD, or GIV-FA (*D*) were stimulated with 50 nM EGF at the indicated time points before lysis. Equal aliquots of whole-cell lysates were analyzed for PKA activity by immunoblotting using anti–phospho-serine/threonine–PKA substrate-specific antibody and tubulin. (*E* and *F*) HeLa cell lysates in *C* and *D* were analyzed for pCREB, phospho-ATF1, and total CREB (tCREB) by immunoblotting and were quantified by band densitometry (Fig. S5 *A* and *B*).

ATF1 (Fig. 4*F* and Fig. S5*B*). By contrast, cells expressing the GDI-deficient GIV-FA mutant (Fig. 4*B*) displayed elevated PKA activity at t15 (Fig. 4*D*) and phosphorylation of CREB and ATF1 at t15 and t30 (Fig. 4*F* and Fig. S5*B*). These analyses revealing contrasting patterns of signaling in control vs. GIV-depleted and in GDI-proficient (GIV-DD) vs. GDI-deficient (GIV-FA) cells demonstrate the role of GIV and its GDI function in the suppression of Gαs GTP→cAMP→PKA→CREB signals.

GIV Promotes Endosomal Maturation and Down-Regulates Mitogenic MAPK→ERK1/2 Signals via Its Ability to Inhibit Gαs. Prior studies (9) have shown that GIV's ability to bind Gαs and the maintenance of Gαs in the inactive state promotes endosomal maturation and thereby accelerates the transit of ligand-activated EGFR through the early endocytic compartment. Conversely, when GIV cannot bind Gαs or when Gαs is active, the transit of ligand-activated EGFR through early endosomes is prolonged. Based on these findings, we expected EGFR trafficking to be accelerated in cells expressing the GDI-proficient GIV-DD mutant, which inhibits Gαs activity, and to be slowed in HeLa cells expressing the GDI-deficient GIV-FA mutant which neither binds nor modulates Gαs signaling. Indeed we found that by t30 ligand-activated autophosphorylated EGFR, as determined by anti-EGFR pY1068, was no longer seen in endosomes expressing early endosome antigen 1 (EEA1) in GIV-WT and GIV-DD cells, but pY1068EGFR still persisted on EEA1$^+$ endosomes in GIV-FA cells (Fig. 5*A*). Together, these findings indicate that the GDI-proficient GIV-DD mutant, which inhibits Gαs activation, ensures rapid clearance of the ligand-activated receptor through endosomes and the finiteness of signaling from that site. By contrast, the GDI-deficient GIV-FA mutant, which impairs binding to Gαs, delays endosomal maturation and prolongs the transit time and signaling from ligand-activated EGFR on EEA1$^+$ endosomes (Fig. 5*A*).

Endosomes are accepted as a legitimate compartment for the propagation of mitogenic MAPK–ERK1/2 signals downstream of growth factors (20, 21). Because GIV's GDI function was required for accelerating the transit time of activated receptors through those compartments, we asked if GIV and, more specifically, its GDI function also affect mitogenic MAPK/ERK1/2 signals. Compared with control cells, GIV-depleted cells showed sustained phosphorylation of ERK1/2 but, as anticipated, failed to enhance phosphorylation of Akt (Fig. 5*B* and Fig. S5*C*). Compared with GIV-WT cells, peak phosphorylation of ERK1/2 was higher in the GDI-deficient GIV-FA cells and was lower in the GDI-proficient GIV-DD cells (Fig. 5*C* and Fig. S5*D*). These findings indicate that GIV requires its GDI function to suppress the MAPK/ERK1/2 signaling axis. Akt phosphorylation, on the other hand, was suppressed in GIV-DD cells compared with GIV-WT cells and, as shown previously (11, 12), was significantly decreased in GIV-FA cells. This result indicates that the GDI-proficient GIV-DD mutant, which does not bind Gαi, can enhance Akt signaling to levels intermediate between those of GIV-WT and GIV-FA. Akt enhancement in the GDI-proficient GIV-DD mutant required free Gβγ, because such activation was inhibited by gallein, a small molecule that blocks Gβγ binding to PI3K (22, 23), but not by fluorescein, its inactive analog (Fig. S6).

Consistent with GDI-proficient GIV-DD cells suppressing and GDI-deficient GIV-FA cells enhancing mitogenic MAPK/ERK and phospho-CREB (pCREB) signals, the rate of proliferation of these cells, as determined by four different approaches—nuclear localization of phosphohistone H3 (Fig. 5*D* and Fig. S7*A*); BrdU uptake (Fig. 5*E* and Fig. S7*B*); cell counting (Fig. 5*F*); and cell viability (Fig. 5*G*) assays—also was decreased in GIV-DD cells by ∼50% compared with GIV-FA cells. These findings support the following model in which EGF stimulation activates both the GEF and GDI functions of GIV via key phosphomodifications flanking the same motif. This bifunctional role of GIV maintains Gαs in the GDP-bound inactive state (Fig. 5*H*); inhibition of Gαs speeds

up endosome maturation and down-regulates mitogenic MAPK–ERK and the cAMP→PKA→CREB signaling axes. Consequently, GIV-dependent inhibition of Gαs primarily suppresses mitosis.

GIV Inhibits Anchorage-Dependent Growth via Its Ability to Inhibit Gαs. Prior studies have demonstrated that the presence or absence of a functional GBA motif in GIV, through which GIV activates Gαi, is a critical determinant of migration–proliferation dichotomy, a hallmark of invasive cancer cells (24). Because the presence or absence of a functional GDI motif in GIV affected the relative levels of motogenic PI3K–Akt signals (which trigger cell migration) and mitogenic MAPK–ERK1/2 signals (which trigger proliferation), we hypothesized that inhibition of Gαs by GIV's GBA motif also contributes to migration–proliferation dichotomy. We found that the

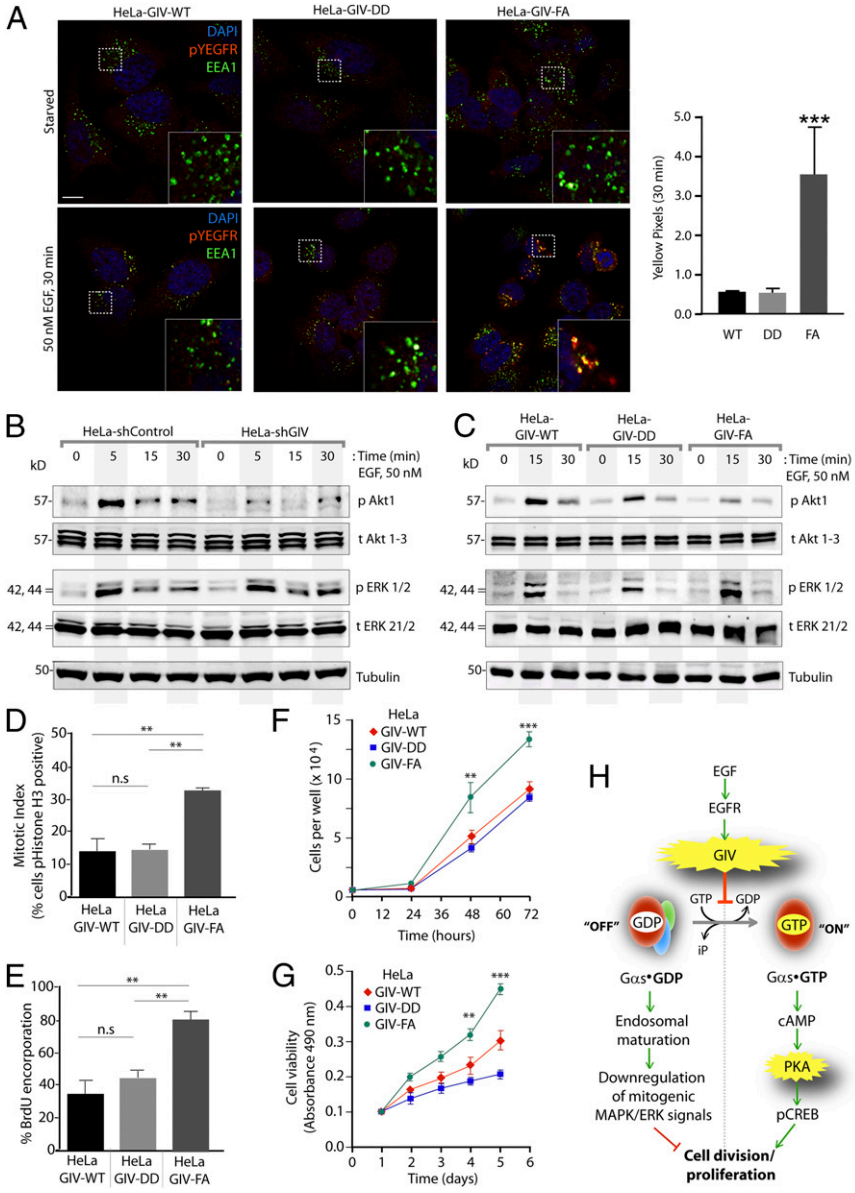

Fig. 5. GIV's ability to bind and inhibit Gαs is essential for EGFR trafficking and down-regulation of mitogenic signals triggered by EGF. (*A*, *Left*) Serum-starved (0.2% FBS, overnight) HeLa cells stably expressing GIV-WT, GIV-DD, or GIV-FA were stimulated with 50 nM EGF for 30 min before fixation. Fixed cells were stained for ligand-activated EGFR (determined by staining for Y1068 phospho-EGFR (pEGFR, Y1068) (red), EEA1 (green), and DAPI (to stain the nucleus; blue) and were examined by confocal microscopy. *Insets* display magnified boxed regions. (Scale bar, 10 μm.) (*Right*) Bar graphs display quantification of yellow pixels indicating colocalization of active EGFR within EEA1$^+$ endosomes in each set of cells at t30. ***$P < 0.001$. (*B* and *C*) Control (shControl) or GIV-depleted (shGIV) HeLa cells (*B*) or GIV-depleted HeLa cells stably expressing GIV-WT, GIV-DD, or GIV-FA mutants (*C*) were starved and stimulated with 50 nM EGF before lysis. Equal aliquots of whole-cell lysates were analyzed for phospho-Akt (pAkt), phospho-ERK (pERK), total Akt (tAkt), total ERK (tERK), and actin by immunoblotting and were quantified by band densitometry (Fig. S5 *C–F*). (*D*) Bar graphs display the mitotic index (*Experimental Procedures*), as determined by the percentage of each HeLa GIV cell line with nuclear phosphorylated (S28)-histone H3 (*y* axis). (*E*) Bar graphs display the percentage of each HeLa GIV cell line stained with anti-BrdU mAb after a BrdU uptake assay. Data in both graphs are presented as mean ± SEM; $n = 3$. **$P < 0.01$. Representative images for *D* and *E* are shown in Fig. S7. (*F* and *G*) Graphs display the rates of proliferation of various GIV HeLa cell lines, as determined by cell counting (*F*) and cell viability assays (*G*). Results are presented as mean ± SEM; $n = 3$. **$P < 0.01$, ***$P < 0.001$. (*H*) Schematic summary of G-protein and EGF signaling data presented in Figs. 3–5. Upon EGF stimulation, GIV serves as a GDI for Gαs and maintains Gαs GDP in the inactive state. (*Left*) The inactive state favors rapid down-regulation of endosome-based mitogenic (MAPK–ERK1/2) signals, as is consistent with prior findings that the presence of inactive Gαs on endosomes accelerates endosomal maturation and EGFR degradation (9). (*Right*) As a direct consequence of GIV-GDI, the Gαs GTP→cAMP→PKA→pCREB signaling pathway is inhibited; this inhibition is a key trigger for cell cycle-progression.

GDI-proficient GIV-DD cells migrated as efficiently as GIV-WT cells, as determined by Transwell chemotaxis assays (Fig. 6 *A* and *B*), but failed to proliferate into colonies, as determined by anchorage-dependent cell growth assays (Fig. 6 *C* and *D*). By contrast, GDI-deficient GIV-FA cells were less motile (Fig. 6 *A* and *B*) and instead preferentially grew into colonies (Fig. 6 *C* and *D*). These results demonstrate that the antiproliferative aspect of migration–proliferation dichotomy requires GIV's ability to inhibit Gαs.

In summary (Fig. 6*E*), we provide evidence that GIV can bind both Gαi and Gαs in a sequential manner after growth factor stimulation. Although binding to both Gα subunits is mediated by the same evolutionarily conserved GBA motif in GIV's C terminus, the binding of the two G proteins has opposite outcomes: GIV serves as a GEF for Gαi and as a GDI for Gαs. Because Gαi and Gαs have opposing roles (inhibitory and stimulatory, respectively) in the regulation of cellular cAMP, GIV's paradoxical ability to activate Gαi and inhibit Gαs results in an overall synergistic down-regulation of cellular cAMP and the cAMP-driven PKA→CREB axis of signaling (Fig. 6*E*). In addition, serving as both a GEF (for Gαi) and a GDI (for Gαs), GIV is capable of releasing free Gβγ heterodimers that can synergistically enhance the Gβγ-driven PI3K→Akt signaling axis (Fig. 6*E*). Although high PI3K–Akt signaling triggers migration, suppression of CREB stalls entry into the cell cycle. We propose that GIV's ability to modulate the two opposing G proteins dually and differentially in a sequential manner is the key property of this signaling circuitry that orchestrates a cohesive, sustained, and robust phenotypic response, one that favors persistent migration without repeated interruption resulting from entry into the cell cycle.

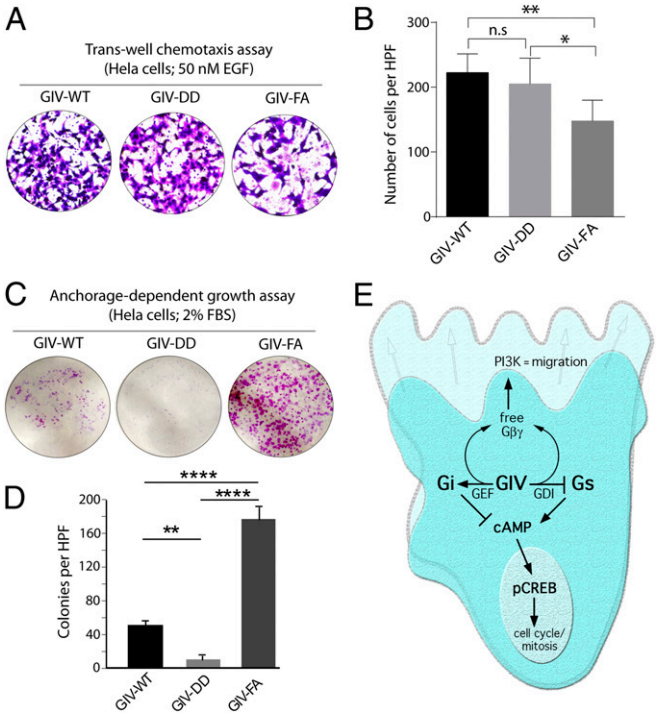

Fig. 6. Inhibition of Gαs signaling by GIV inhibits anchorage-dependent tumor growth but does not affect cell motility/chemotaxis in HeLa cells. (*A* and *B*) GIV HeLa cell lines were analyzed for chemotaxis toward EGF using a Transwell migration assay (*Experimental Procedures*). After 6 h, membranes were fixed and stained with toluidine blue and imaged at 20×. (*A*) Representative images of high-power fields (HPF). (*B*) Bar graphs display the number of migrating cells per HPF (*y* axis) averaged from 20 HPFs per experiment; $n = 3$. Data are presented as mean ± SEM; $^{*}P < 0.05$, $^{**}P < 0.01$. (*C* and *D*) The HeLa cell lines used in *A* were analyzed for anchorage-dependent growth on six-well plastic plates (*Experimental Procedures*). After 2 wk, cells were fixed and stained with crystal violet. (*C*) Representative images of the crystal violet-stained single wells of a six-well plate. (*D*) Bar graphs display the average number of colonies per HPF (*y* axis), as determined using the colony-counter feature of ImageJ; colonies in 20 HPFs per well from two wells per experiment were counted, $n = 4$. Results are expressed as ± SEM; $^{**}P < 0.01$, $^{****}P < 0.0001$. (*E*) Schematic summarizing the findings of the current work integrated with previous literature on GIV's role in the modulation of G-protein and growth factor signaling during cell migration. Previously published work (on the left) has shown that GIV triggers the activation of Gαi via an evolutionarily conserved, C-terminally located GBA motif (1). Activation of Gi has two major consequences: (*i*) free Gβγ heterodimers released from Gi activate the PI3K–Akt pathway (1), and (*ii*) activation of Gαi suppresses cellular cAMP (7). This work (on the right) shows that GIV's GBA motif also serves as a GDI for Gαs and maintains the G protein in an inactive Gαs-GDP state. Inhibition of Gαs by GIV also releases free Gβγ (Fig. S6) and suppresses cellular cAMP, thereby synergistically potentiating both consequences of Gαi activation. Overall, GIV's GBA motif suppresses mitogenic MAPK/ERK1/2 signals and cAMP→pCREB–mediated cell-cycle progression and enhances promigratory PI3K–Akt signals by paradoxically activating and inhibiting two opposing G proteins.

Discussion

One Motif Serves as a GEF and GDI: Genesis of Pleiotropy in G-Protein Signaling. The major finding in this work is the identification of GIV as a GDI for Gαs. Together with its previously well-characterized ability to bind Gαi (1, 25, 26), GIV joins several other receptor GEFs, i.e., GPCRs (27–30), that can dually couple to both Gi and Gs, two G proteins with opposing effects on adenylyl cyclase and the generation of cellular cAMP. In all instances in which dual coupling of GPCRs to Gi and Gs has been reported, ligand stimulation leads to the activation of both G proteins. By contrast, GIV appears to be a unique modulator that can modulate the two G proteins paradoxically, activating Gαi and inactivating Gαs.

A series of studies (reviewed in ref. 31) has established GIV as a bona fide GEF for Gαi. Here, using enzymatic assays with recombinant proteins, we show that GIV inhibits the rate of Gαs nucleotide exchange. Consistent with the properties of other known GDIs, prior studies have confirmed that GIV cannot bind Gαs subunits in the active GTP-bound conformation (9–11). It is noteworthy that both the GEF and GDI functions of GIV are mediated via the same evolutionarily conserved C-terminal short GBA motif, as reported previously in the case of the synthetic KB-752 peptide (14, 15). Such a role is analogous to the bifunctional [GTPase-activating proteins (GAP) and GDI] role of the regulators of G protein signaling (or RGS) domain of *Drosophila* Double hit (Dhit) (32).

How can the same motif serve as both a GEF and a GDI? Although mechanistic insights are lacking at the atomic level, multiple studies (1, 26, 33) have provided important structural insights into the assembly of the GIV–Gα complex by using a combination of homology modeling [based on the X-ray structure of the KB-752 peptide bound to Gαi1 (14)] and site-directed mutagenesis (1, 17). These studies have revealed that conserved hydrophobic residues that align on one side of a short aliphatic helix in GIV dock onto a hydrophobic cleft between the switch II and the α3 helix of Gαi/s. The structure of the KB-752 peptide-bound Gαi1 (14) also sheds light on how the homologous short stretch in GIV can accelerate nucleotide exchange rates of Gαi subunits: The peptide appears to alter switch I and II regions of Gαi, which were proposed to create a feasible exit route for GDP (14). Thus, well-validated homology models of GIV-bound Gαi3 built using the KB-752–bound Gαi1 as a template allow us to rationalize how GIV, like the KB-752 peptide, serves as a GEF for Gαi subunits. By contrast, as yet we have no clear rationale as to why GIV may serve as a GDI for Gαs. That both the KB-752 peptide (15) and GIV do exert a GDI-like effect on Gαs suggests that both may inhibit one or more of the conformational steps believed to facilitate GDP release by Gαs (34), i.e., unhinging of the Ras-like and helical domains, destabilization of the GDP-binding site, or movement of the α5-helix and/or the α4–β6 loop.

Insight at an atomic level by X-ray crystallography is required to resolve this question.

Finally, in light of the findings of this work, we propose a nomenclature, "guanine-nucleotide exchange modulators" (GEMs), to describe the GIV family of G-protein modulators, all of which share homology with the KB-752 peptide. GEMs such as GIV or the synthetic KB-752 peptide are distinct from the other nonreceptor GEFs (such as Ric8A/B or AGS1) because they have a well-defined GBA motif (35) that can display a propensity for pleiotropy; i.e., the motif can either accelerate or inhibit nucleotide exchange and thereby serve as a GEF or a GDI, depending on the G-protein substrate and posttranslational modifications flanking the motif. Whether other GIV-related G-protein regulators, such as Daple (36) and Calnuc (35), which serve as GEFs for Gαi via GBA motifs that are similar to those in KB-752 and GIV, also serve as GDIs for Gαs remains to be explored.

Two Key Phosphoevents Shift GIV's Preference from Gαi to Gαs. Another finding in this work is the sequential nature of GIV–Gαi and GIV–Gαs interactions after ligand stimulation. GIV–Gαi complexes are assembled within 5 min and are disassembled ∼15–30 min after EGF stimulation. Although their assembly is triggered by phosphorylation of GIV at S1674, an event catalyzed by CDK5 within seconds to minutes after EGF stimulation (11), their disassembly is triggered by phosphorylation of GIV at S1689, an event catalyzed by PKCθ (13). GIV–Gαs complexes are assembled at approximately t15–t30 and are disassembled by approximately t60 after EGF stimulation, coinciding with the abundance of phosphorylation of GIV at S1689. Because GIV phosphorylated at S1674 binds both Gαi and Gαs but has an ∼5- to 10-fold higher affinity for Gαi, and because GIV that is dually phosphorylated at S1674 and S1689 can bind only Gαs, it is likely that the second phosphoevent (at S1689 catalyzed by PKCθ) is the key trigger that shifts GIV's preference from Gαi to Gαs. We conclude that two sequential phosphomodifications on GIV that are catalyzed by two kinases, CDK5 and PKCθ, ensure that GIV exerts its GEF and GDI activities on Gαi and Gαs, respectively, in a temporally and spatially segregated manner.

Pleiotropic G-Protein Signaling Triggered by GIV Integrates Downstream Signals and Reinforces a Promigratory Phenotype. We also show here the consequences of Gi activation and Gs inhibition by GIV on downstream signaling pathways and the cellular response to growth factors. Previous studies have shown that binding and activating Gαi prolongs the time that EGFRs spend on the cell surface and enhances PM-based promigratory PI3K–Akt signals (12). Binding Gαs, on the other hand, and maintaining it in the GDP-bound inactive state shortens the time EGFRs spend in endosomes and diminishes the endosome-based promitotic Ras/Raf/MAPK/ERK pathway (9). Consequently, when GIV's GBA motif can bind and modulate both Gα subunits, cells enhance PI3K–Akt signals from the PM and suppress mitogenic MAPK–ERK1/2 signals from endosomes by ensuring rapid transit through endocytic compartments; as a consequence, cells preferentially migrate and suppress proliferation. When GIV's GBA motif cannot bind or modulate either G protein, cells suppress PI3K–Akt signals at the PM and enhance mitogenic MAPK–ERK1/2 signals from endosomes by delaying the transit time of EGFR through endocytic compartments; consequently, cells are poorly motile and preferentially divide. This phenotype is seen in cells expressing either GIV-FA or GIV-74A, a mutant that cannot be phosphorylated by CDK5 and therefore cannot bind either G protein in cells (11). Because the inhibitory effects of GIV-WT on Gαs activity, on mitogenic MAPK–ERK1/2 signals, and on cell proliferation can be fully recapitulated in cells expressing GIV-DD, a phosphomutant that exclusively binds and inhibits Gαs but cannot bind or activate Gαi, we conclude that the GIV's ability to bind and inhibit Gαs is required and is primarily responsible for GIV's antiproliferative effects.

What is the primary role of GIV's ability to bind and activate Gαi? Although a mutant GIV that can bind and activate Gαi but cannot bind and inhibit Gαs is yet to be identified, the role of Gi activation by GIV is apparent from a subtractive analysis of readouts of GIV-WT cell lines, which can modulate both Gi/s, vs. phosphomutant GIV-DD cell lines, which can modulate only Gs. Such analysis shows that the cells expressing the GIV-DD mutant have an intermediate level of peak Akt phosphorylation, lower than that of GIV-WT, which has an intact GBA motif, but higher than that of GIV-FA, which has no functional GBA motif (Fig. S5*D*). This finding indicates that GIV's ability to inhibit Gαs can account for only part of the observed role of GIV's GBA motif in the enhancement of Akt signals and that activation of Gi is the likely contributor of the remaining part. Because GIV displaces Gβγ from Gαs (Fig. S6*A*) and because Akt signals enhanced by GIV's GBA motif are inhibited by gallein (Fig. S6*B*) (1), a compound that blocks Gβγ interactions with PI3Kγ by binding to a protein–protein interaction hot spot on the Gβ subunit (22), we conclude that the mechanism of PI3K–Akt enhancement brought about by GIV's GBA motif involves the release of free Gβγ heterodimers from both Gi and Gs trimers. Thus, by triggering the activation of Gi and inhibiting Gs, GIV accomplishes one common goal, i.e., the release of free Gβγ and the activation of PI3K–Akt signals, thereby integrating and reinforcing the downstream signaling response (Fig. 6*E*).

Another final common goal that can be accomplished by the paradoxical activation of Gi and inhibition of Gs is the suppression of cellular cAMP. Prior studies using a FRET-based approach have confirmed that activation of Gi by GIV is critical for the suppression of cellular cAMP at approximately t5 in cells pretreated with forskolin (7). Analyses of signaling pathways in control vs. GIV-depleted cells responding to EGF underscore the importance of GIV in suppressing both PKA activation and the phosphorylation of CREB by approximately t5 and continuing to do so up to approximately t30–t45. This timeline suggests that much of the early suppression of the cAMP→PKA→pCREB axis we observe is likely to be contributed by GIV-dependent activation of Gαi, which occurs early (at approximately t5) and excludes any significant contribution from GIV-dependent inhibition of Gαs which occurs later (at approximately t15–t30). Conversely, the sustained suppression of the cAMP→PKA→pCREB axis until t30–t45 is likely contributed exclusively by the GIV-dependent inhibition of Gαs, because GIV can no longer bind or activate Gαi at these delayed time points. We propose that by triggering paradoxical activation of Gi and inhibition of Gs, GIV's GBA motif integrates and reinforces another common goal, the suppression of the cAMP→PKA→pCREB axis (Fig. 6*E*).

We propose that the cellular response to paradoxical signaling that is triggered by GIV is likely to be shaped by both the sequential and spatiotemporally segregated nature of GIV-dependent modulation of Gαi and Gαs: The sequential triggering likely ensures pulses of early (Gαi-dependent) and late (Gαs-dependent) signals, whereas the spatiotemporally segregated triggering likely ensures the compartmentalization of those pulses.

In conclusion, we provide evidence of pleiotropic G-protein signaling in physiology in which one protein can both accelerate and inhibit the guanine nucleotide exchange rates of two opposing G proteins, Gαi and Gαs, using the same module. These insights provide clues into how GIV may achieve sustained and coordinated responses through pulses of compartmentalized signals.

Experimental Procedures

Detailed methods are described in *SI Experimental Procedures*.

Cell Culture, Transfection, Immunoblotting, Immunofluorescence, and Protein–Protein Interaction Assays (GST Pulldowns and Immunoprecipitations). Cell culture, transfection, immunoblotting, immunofluorescence, and protein–protein interaction assays were carried out exactly as described previously (1, 9, 11, 12, 33). All transfections were performed using *Trans*IT-LT1 reagent (Mirus Bio). All Western

blotting (Odyssey–LI-COR) images were processed and assembled for presentation using Image Studio Lite, Photoshop, and Illustrator software (Adobe).

PLA. In situ interactions of endogenous GIV with Gαi3 or Gαs were detected using a Duolink proximity ligation assay kit (Olink Bioscience) per the manufacturer's instructions, as done previously (11).

Single-Turnover and Steady-State GTPase Assays. Single-turnover and steady-state GTPase assays were performed as described previously (26, 37), with minor modifications outlined in *SI Experimental Procedures*.

Live-cell imaging for visualizing Gαs activation using conformational-specific GFP nanobodies on HeLa cells was done using a PerkinElmer spinning disk confocal microscope as described previously (17).

BrdU Incorporation, Phosphohistone H3 Staining, and Estimation of Mitotic Index. BrdU incorporation, phosphohistone H3 staining, and estimation of mitotic index were performed as described previously (9, 11, 12).

Anchorage-Dependent Colony Formation Assay. Anchorage-dependent growth was monitored on a solid (plastic) surface as described previously (11). Briefly, 1,000 GIV-depleted HeLa cells stably expressing WT, 74D, and 74A GIV-FLAG constructs were grown in six-well tissue-culture plates at 37 °C for 2 wk in medium supplemented with 0.2% FBS before staining with 0.005% crystal violet for 1 h. Images were acquired by light microscopy.

Transwell Migration Assay. Transwell migration assays were carried out using Costar Transwell inserts with 8-μm pores in 24-well plates exactly as described previously (11).

Statistical Analysis. Each experiment presented in the figures is representative of at least three independent experiments. Statistical significance between the differences of means was calculated by unpaired Student's *t* test. A two-tailed *P* value of < 0.05 at a 95% confidence interval is considered statistically significant; $*P < 0.05$, $**P < 0.01$, $***P < 0.001$, $****P < 0.0001$. All graphical data presented were prepared using GraphPad or Matlab software.

ACKNOWLEDGMENTS. This work was supported by NIH Grants CA100768 (to M.G.F. and P.G.) and CA160911 and DK099226 (to P.G.). Support was also provided by a Career Award for Medical Scientists award from the Burroughs Wellcome Fund (to P.G.); American Cancer Society Grant ACS-IRG 70-002 (to P.G.); the Moores Cancer Center of the University of California, San Diego (P.G.); American Cancer Society Grant RSG-13-362-01-TBE (to M.G.-M.); NIH Grant R01GM108733 (to M.G.-M.); Susan G. Komen Grant PDF14298952 (to K.K.M.); and American Heart Association Fellowship AHA 14POST20050025 (to I.L.-S.). D.B. was supported by NIH Building Infrastructure Leading to Diversity (BUILD) Research Stimulation Grant (UL1MD009601) and California State University Program for Education and Research in Biotechnology (CSUPERB) New Investigator Grant (GF00631143).

1. Garcia-Marcos M, Ghosh P, Farquhar MG (2009) GIV is a nonreceptor GEF for G alpha i with a unique motif that regulates Akt signaling. *Proc Natl Acad Sci USA* 106(9): 3178–3183.
2. Enomoto A, et al. (2005) Akt/PKB regulates actin organization and cell motility via Girdin/APE. *Dev Cell* 9(3):389–402.
3. Anai M, et al. (2005) A novel protein kinase B (PKB)/AKT-binding protein enhances PKB kinase activity and regulates DNA synthesis. *J Biol Chem* 280(18):18525–18535.
4. Ghosh P (2015) G protein coupled growth factor receptor tyrosine kinase: No longer an oxymoron. *Cell Cycle* 14(16):2561–2565.
5. Aznar N, Kalogriopoulos N, Midde KK, Ghosh P (2016) Heterotrimeric G protein signaling via GIV/Girdin: Breaking the rules of engagement, space, and time. *BioEssays* 38(4):379–393.
6. Lin C, et al. (2014) Structural basis for activation of trimeric Gi proteins by multiple growth factor receptors via GIV/Girdin. *Mol Biol Cell* 25(22):3654–3671.
7. Midde KK, et al. (2015) Multimodular biosensors reveal a novel platform for activation of G proteins by growth factor receptors. *Proc Natl Acad Sci USA* 112(9):E937–E946.
8. Lin C, et al. (2011) Tyrosine phosphorylation of the Gα-interacting protein GIV promotes activation of phosphoinositide 3-kinase during cell migration. *Sci Signal* 4(192):ra64.
9. Beas AO, et al. (2012) Gαs promotes EEA1 endosome maturation and shuts down proliferative signaling through interaction with GIV (Girdin). *Mol Biol Cell* 23(23):4623–4634.
10. Le-Niculescu H, Niesman I, Fischer T, DeVries L, Farquhar MG (2005) Identification and characterization of GIV, a novel Galpha i/s-interacting protein found on COPI, endoplasmic reticulum-Golgi transport vesicles. *J Biol Chem* 280(23):22012–22020.
11. Bhandari D, et al. (2015) Cyclin-dependent kinase 5 activates guanine nucleotide exchange factor GIV/Girdin to orchestrate migration-proliferation dichotomy. *Proc Natl Acad Sci USA* 112(35):E4874–E4883.
12. Ghosh P, et al. (2010) A Galphai-GIV molecular complex binds epidermal growth factor receptor and determines whether cells migrate or proliferate. *Mol Biol Cell* 21(13):2338–2354.
13. López-Sánchez I, et al. (2013) Protein kinase C-theta (PKCθ) phosphorylates and inhibits the guanine exchange factor, GIV/Girdin. *Proc Natl Acad Sci USA* 110(14):5510–5515.
14. Johnston CA, et al. (2005) Structure of Galpha(i1) bound to a GDP-selective peptide provides insight into guanine nucleotide exchange. *Structure* 13(7):1069–1080.
15. Johnston CA, et al. (2005) A bifunctional Galphai/Galphas modulatory peptide that attenuates adenylyl cyclase activity. *FEBS Lett* 579(25):5746–5750.
16. Söderberg O, et al. (2006) Direct observation of individual endogenous protein complexes in situ by proximity ligation. *Nat Methods* 3(12):995–1000.
17. Irannejad R, et al. (2013) Conformational biosensors reveal GPCR signalling from endosomes. *Nature* 495(7442):534–538.
18. Klarenbeek JB, Goedhart J, Hink MA, Gadella TW, Jalink K (2011) A mTurquoise-based cAMP sensor for both FLIM and ratiometric read-out has improved dynamic range. *PLoS One* 6(4):e19170.
19. Ponsioen B, et al. (2004) Detecting cAMP-induced Epac activation by fluorescence resonance energy transfer: Epac as a novel cAMP indicator. *EMBO Rep* 5(12):1176–1180.
20. Haugh JM (2002) Localization of receptor-mediated signal transduction pathways: The inside story. *Mol Interv* 2(5):292–307.
21. Murphy JE, Padilla BE, Hasdemir B, Cottrell GS, Bunnett NW (2009) Endosomes: A legitimate platform for the signaling train. *Proc Natl Acad Sci USA* 106(42):17615–17622.
22. Bonacci TM, et al. (2006) Differential targeting of Gbetagamma-subunit signaling with small molecules. *Science* 312(5772):443–446.
23. Lehmann DM, Seneviratne AM, Smrcka AV (2008) Small molecule disruption of G protein beta gamma subunit signaling inhibits neutrophil chemotaxis and inflammation. *Mol Pharmacol* 73(2):410–418.
24. Fedotov S, Iomin A (2007) Migration and proliferation dichotomy in tumor-cell invasion. *Phys Rev Lett* 98(11):118101.
25. Garcia-Marcos M, et al. (2012) Functional characterization of the guanine nucleotide exchange factor (GEF) motif of GIV protein reveals a threshold effect in signaling. *Proc Natl Acad Sci USA* 109(6):1961–1966.
26. Garcia-Marcos M, Ghosh P, Ear J, Farquhar MG (2010) A structural determinant that renders G alpha(i) sensitive to activation by GIV/girdin is required to promote cell migration. *J Biol Chem* 285(17):12765–12777.
27. Xiao RP (2001) Beta-adrenergic signaling in the heart: Dual coupling of the beta2-adrenergic receptor to G(s) and G(i) proteins. *Sci STKE* 2001(104):re15.
28. Herrlich A, et al. (1996) Involvement of Gs and Gi proteins in dual coupling of the luteinizing hormone receptor to adenylyl cyclase and phospholipase C. *J Biol Chem* 271(28):16764–16772.
29. Michal P, Lysíková M, Tucek S (2001) Dual effects of muscarinic M(2) acetylcholine receptors on the synthesis of cyclic AMP in CHO cells: Dependence on time, receptor density and receptor agonists. *Br J Pharmacol* 132(6):1217–1228.
30. Bonhaus DW, Chang LK, Kwan J, Martin GR (1998) Dual activation and inhibition of adenylyl cyclase by cannabinoid receptor agonists: Evidence for agonist-specific trafficking of intracellular responses. *J Pharmacol Exp Ther* 287(3):884–888.
31. Garcia-Marcos M, Ghosh P, Farquhar MG (2015) GIV/Girdin transmits signals from multiple receptors by triggering trimeric G protein activation. *J Biol Chem* 290(11): 6697–6704.
32. Lin C, et al. (2014) Double suppression of the Gα protein activity by RGS proteins. *Mol Cell* 53(4):663–671.
33. Garcia-Marcos M, Ear J, Farquhar MG, Ghosh P (2011) A GDI (AGS3) and a GEF (GIV) regulate autophagy by balancing G protein activity and growth factor signals. *Mol Biol Cell* 22(5):673–686.
34. Dror RO, et al. (2015) Signal transduction. Structural basis for nucleotide exchange in heterotrimeric G proteins. *Science* 348(6241):1361–1365.
35. Garcia-Marcos M, Kietrsunthorn PS, Wang H, Ghosh P, Farquhar MG (2011) G Protein binding sites on Calnuc (nucleobindin 1) and NUCB2 (nucleobindin 2) define a new class of G(alpha)i-regulatory motifs. *J Biol Chem* 286(32):28138–28149.
36. Aznar N, et al. (2015) Daple is a novel non-receptor GEF required for trimeric G protein activation in Wnt signaling. *eLife* 4:e07091.
37. Leyme A, Marivin A, Casler J, Nguyen LT, Garcia-Marcos M (2014) Different biochemical properties explain why two equivalent Gα subunit mutants cause unrelated diseases. *J Biol Chem* 289(32):21818–21827.
38. Yost EA, Mervine SM, Sabo JL, Hynes TR, Berlot CH (2007) Live cell analysis of G protein beta5 complex formation, function, and targeting. *Mol Pharmacol* 72(4): 812–825.
39. Schnölzer M, Alewood P, Jones A, Alewood D, Kent SB (1992) In situ neutralization in Boc-chemistry solid phase peptide synthesis. Rapid, high yield assembly of difficult sequences. *Int J Pept Protein Res* 40(3-4):180–193.